



TITLE:

Large-scale climatic teleconnection for predicting extreme hydro-climatic events in southern Japan

AUTHOR(S):

Kantoush, Sameh; Nourani, Vahid

CITATION:

Kantoush, Sameh ...[et al]. Large-scale climatic teleconnection for predicting extreme hydro-climatic events in southern Japan. 2023: 共同研究（長期滞在型）2022L-04.

ISSUE DATE:

2023

URL:

<http://hdl.handle.net/2433/285705>

RIGHT:



Disaster Prevention Research Institute
Kyoto University

2022L-04

Large-scale climatic teleconnection for predicting extreme hydro-climatic events in southern Japan

Coordinator: Sameh Kantoush

Prncipial Invistegator: Vahid Nourani

1. Introduction

Oceanic-Atmospheric Teleconnection Patterns (OATPs) are large-scale climate patterns that link atmospheric and oceanic circulations over different regions of the Earth. These patterns play a crucial role in influencing global weather and climate variability. OATPs are typically characterized by fluctuations in sea surface temperatures (SST), atmospheric pressure, wind patterns, and precipitation. Oceanic-atmospheric teleconnection patterns could affect hydro-climatic events over large distances across the world. Accurately predicting hydro-climatic events (such as maximum precipitation or drought events) can help decision-makers improve planning to mitigate the adverse impacts and take advantage of beneficial conditions (Dhanya & Nagesh Kumar, 2009; Moser & Hart, 2015). About some well-known examples of OATPs, it can be referred to as El Niño-Southern Oscillation (ENSO), North Atlantic Oscillation (NAO), Pacific Decadal Oscillation (PDO), and Indian Ocean Dipole (IOD). ENSO is one of the most prominent OATPs, involving interactions between the tropical Pacific Ocean and the overlying atmosphere. It consists of two phases: El Niño and La Niña. During El Niño, the central and eastern tropical Pacific experiences warmer-than-normal sea surface temperatures, while cooler-than-normal sea surface temperatures characterize La Niña. ENSO impacts weather and climate globally, influencing rainfall patterns, temperature anomalies, and storm tracks. NAO is an OATP that influences weather patterns in the North Atlantic region. It involves fluctuations in atmospheric pressure differences between the Icelandic Low and the Azores High. Positive NAO phases are associated with stronger westerly winds, milder winters in Europe, and increased storm activity, while negative phases lead to colder winters and reduced storm activity. PDO is a longer-term OATP that influences the Pacific Ocean's sea surface temperatures and atmospheric circulation patterns. It operates on a decadal time scale, with positive phases characterized by warm SST anomalies along the western coast of North America and cool anomalies in the central Pacific, and vice versa for negative phases. PDO can impact weather patterns and marine ecosystems in the Pacific. IOD is an OATP that occurs in the Indian Ocean. It involves the interaction between temperature gradients in the western and eastern parts of the basin. Positive IOD phases are characterized by warmer-than-normal sea surface temperatures in the western Indian Ocean and cooler-than-normal temperatures in the eastern Indian Ocean, resulting in shifts in rainfall patterns in surrounding regions.

From the early 1900s, various climatic and oceanic parameters have been used to predict hydro-climatic events. Thus, if the association of the hydro-climatic events with the climatic and oceanic parameters is identified, this can be used for designing an effective risk management system for facing the extremes of adverse impacts (Webster et al., 1998). For example, the influence of persistent positive phases of the North Atlantic Oscillation (NAO) on Romania's drought was reported by Stefan et al. (2004). The spatial and temporal variability of the river discharges and precipitation from the southern part of Romania for 69 years, during 1931–99, is investigated. The study is based on river discharge (precipitation) data recorded at ten hydrometric and six meteorological stations from this region. The cross-correlation analysis reveals a seasonal

dependence of the lag time between the precipitation and river discharge anomalies, being larger in winter than in summer. In the research by Ghasemi & Khalili (2008), the wet conditions in Iran were found to be characterized by a negative SST anomaly in the Mediterranean and the Black Sea, while dry conditions were found to be characterized by a positive SST anomaly in the Mediterranean and the Black Sea. The substantial link between southwest Iran's streamflow and the Mediterranean Sea's sea surface temperature (SST) was reported by Meidani & Araghinejad (2014). The influence of the Pacific Decadal Oscillation (PDO) on drought conditions in the United States was reported by Wang et al. (2015), which examined the association between PDO phases and the occurrence and severity of drought events across different regions of the country. Research has shown that the combined effects of PDO and ENSO can significantly impact global land dry-wet changes. For example, during positive PDO and El Niño phases, there tends to be increased rainfall in the western United States and decreased rainfall in Australia and Indonesia. Conversely, during negative PDO and La Niña phases, there tends to be decreased rainfall in the western United States and increased rainfall in Australia and Indonesia. These patterns can significantly impact agriculture, water resources, and other human and natural systems aspects. The influence of regional SST variations on tropic rainfall was recently reported by Ying et al. (2019). In such research, the ocean-atmospheric factors are important in coping with hydro-climatic occurrences.

Extreme events such as heavy rainfall occasionally cause flooding and have severe socio-economic impacts. For example, in early July 2018, extremely heavy rainfall seriously impacted southern Japan. Oceanic-atmospheric teleconnection patterns could affect hydro-climatic events over large distances across the world. Accurately predicting hydro-climatic events can help decision-makers improve planning to mitigate the adverse impacts and take advantage of beneficial conditions (Dhanya & Nagesh Kumar, 2009; Moser & Hart, 2015). Thus, if the association of the hydro-climatic events with the climatic and oceanic parameters is identified, this can be used for designing an effective risk management system for facing the extremes of adverse impacts (Webster et al., 1998).

Traditional approaches (e.g., linear and nonlinear regression or correlation) were employed in the studies mentioned above (as well as most prior efforts) merely to uncover the possible teleconnection between hydro-climatic parameters, and almost no prediction has been made. However, to deal with large-scale hydro-climatic events with highly uncertain circumstances (e.g., maximum monthly precipitation) and to predict their long-term states, Fuzzy Logic (FL) approaches might be an excellent alternative to traditional methods since they might partially represent such uncertainty (Dhanya & Nagesh Kumar, 2009; Nourani et al., 2021). The FL has recently been widely applied to analyze complex processes owing to its high capacity to handle

system uncertainty, which is frequent in hydro-climatic modeling (Nourani et al., 2014; He et al., 2019; Najafi et al., 2022). The FL models can effectively determine aspects of data that are not clearly defined or fundamentally certain. To model with fuzzy logic methods, it is essential to determine the if-then rules. Constructing if-then rules is difficult due to the intricacy and uncertainty of far-away teleconnection mechanisms. In this regard, data mining (e.g., association mining) can be appropriate for extracting the patterns and constructing if-then rules (Tadesse et al., 2004). For example, Dadaser-Celik et al. (2013) utilized association mining to investigate the connections between streamflow and meteorological factor for Kzlrnak River Basin in Turkey.

The principal problem of the classic fuzzy-based method is its weakness when dealing with the vague conditions often involved in realistic settings. Despite the widespread application of the classic FL concept, discussing the confidence and reliability of the analyzed information is critical because the classic fuzzy variables only include constraints and do not provide reliability. Generally, some words are often used to describe variables. For example, when it is said that "the weather outside is cold" or equivalently, "the air temperature outside is low," the word "low" is used to describe the "air temperature outside." The variable "outside air temperature" has accepted the word "low" as its value. Accordingly, outside temperature can take values such as 0° , -4° , -7° , etc. The FL considers a particular range for low temperature, which shows the constraints of that variable (for example, between 0° to -7°). The conventional FL only includes constraints and does not provide reliability, so it can partially reflect such uncertainty. For example, in the FL, when it is said, "If the temperature is high, the evaporation will be high," how much confidence is there that the temperature is high?

Since traditional fuzzy techniques merely contain restrictions and do not give reliability, it is important to discuss the reliability of the studied data. In this regard, researchers are now interested in Zadeh's proposal for Z-number, introduced in 2011. For instance, "If the temperature is very high, which usually happens in summer, most probably the evaporation will be high." (usually happens) and (most probably) are the reliable parts of the temperature and evaporation, respectively. The reliability part of the Z-number approach refers to the accuracy of both input variables and rules, and it is the main difference between fuzzy and Z-number models. The Z-numbers can provide valuable insight into experts' uncertainty in engineering problems because they depend on constraints and the reliability of the information (Akbarian Saravi et al., 2019; Aboutorab et al., 2018). For example, Nourani et al. (2021) and Najafi et al. (2022) used the Z-

number Based Model (ZBM) for drought monitoring and precipitation modeling, respectively, using large-scale oceanic-atmosphere teleconnections. Maleki et al. (2023) also utilized a Z-number approach to assess groundwater-specific vulnerability, including DRASTIC parameters and nitrate concentrations. The results revealed that the Z-number could provide reliable estimations since it could consider the reliability and uncertainty of data and allocate proper weight for the rules. This research study will focus on developing the Z-number-based model to predict extreme weather events in southern Japan.

Determining the if-then rules to model with fuzzy logic methods (and the Z-number approach) is essential. Constructing if-then rules with traditional methods is complicated due to the intricacy and uncertainty of far-away teleconnection mechanisms. In this regard, data mining (e.g., association mining) can be appropriate for extracting patterns and constructing if-then rules (Tadesse et al., 2004). For example, Dadaser-Celik et al. (2013) utilized association mining to investigate the connections between streamflow and meteorological factors in Turkey's Kizilirmak River Basin. It is possible to analyze uncertain processes using data mining by generating rules which display the cause-effect relation between different combinations of the hydroclimatic parameters (e.g., see, Nourani et al., 2021; Najafi et al., 2022; Maleki et al., 2023).

Large-scale ocean-atmospheric signals such as the Southern Oscillation Index (SOI), ENSO, sea surface temperature (SST) of surrounding seas, etc., could affect extreme weather events over southern Japan (e.g., see Kosaka and Nakamura, 2010; Ohba & Sugimoto, 2021). Most prior efforts, such as Ohba and Sugimoto (2021), merely investigated the possible teleconnection between hydro-climatic parameters. The study focuses on the winter season in Japan and aims to understand the mechanisms by which ENSO affects precipitation in the region. The study used a combination of observational data and model simulations to analyze the frequency and precipitation of synoptic weather patterns associated with ENSO. The finding shows that dynamic and thermodynamic processes contribute to the ENSO-related precipitation variability in Japan. The dynamic process involves changes in the atmospheric circulation patterns, while the thermodynamic process involves changes in the atmosphere's moisture content. The study also identifies synoptic weather patterns associated with ENSO-related precipitation anomalies in Japan, such as the East Asian winter monsoon and the Pacific-Japan pattern.

However, in their study, almost no prediction has been made. So, by extracting the possible teleconnection, this research will predict the occurrence of extreme events. In this regard, because of the complexity and uncertainties of the teleconnection processes, this research investigated the ZBM performance in predicting Japan's classified hydro-climatic events. To this end, the ocean-atmospheric signals, such as the SST of adjacent seas, will use as predictors.

In the following the contributions and innovations of this research are summarized:

1. This research, by evaluating the data reliability, will investigate the use of oceanic-atmospheric signals as predictors to predict hydro-climatic extreme events.
2. In the suggested Z-number-based-model, to prevent the loss of some information, a Z-number will directly use for computation.
3. This research proposes the association mining tool to extract (explain) the teleconnection pattern between hydro-climatic parameters and the construction of if-then rules.

2. Study area

Japan has a diverse climate influenced by its geographic location, topography, and the surrounding ocean currents. Generally, Japan experiences four distinct seasons: spring, summer, autumn, and winter. Spring (March to May): Spring in Japan is mild and considered one of the best seasons to visit. Temperatures gradually rise, with an average range of 10°C to 20°C (50°F to 68°F). Summer (June to August): Summers in Japan are generally hot and humid, particularly in July and August. Average temperatures range from 25°C to 35°C (77°F to 95°F), but they can sometimes reach higher temperatures. The summer season also brings the rainy season (known as "Tsuyu" or "Baiu") in June and July, characterized by frequent rainfall. Autumn (September to November): Autumn in Japan is known for its vibrant fall foliage, especially in mountainous regions. The weather is generally mild and pleasant, with temperatures ranging from 15°C to 25°C (59°F to 77°F). Winter (December to February): Winters in Japan vary depending on the region. Northern areas, such as Hokkaido, experience cold temperatures and heavy snowfall. In central and southern parts, including Tokyo and Kyoto, winters are milder but can still be chilly, with temperatures ranging from 0°C to 10°C (32°F to 50°F). Typhoon Season: Japan is also prone to typhoons, which usually occur between May and October. These powerful tropical cyclones can bring heavy rains,

strong winds, and disruption to transportation and daily life. Northern Japan has warm summers and very cold winters with heavy snow. Eastern Japan has hot and humid summers and cold winters with very heavy snow. Western Japan has very hot and humid summers and moderately cold winters. Okinawa and Amami (southern Japan) have hot and humid summers and mild winters (see Figure 1).

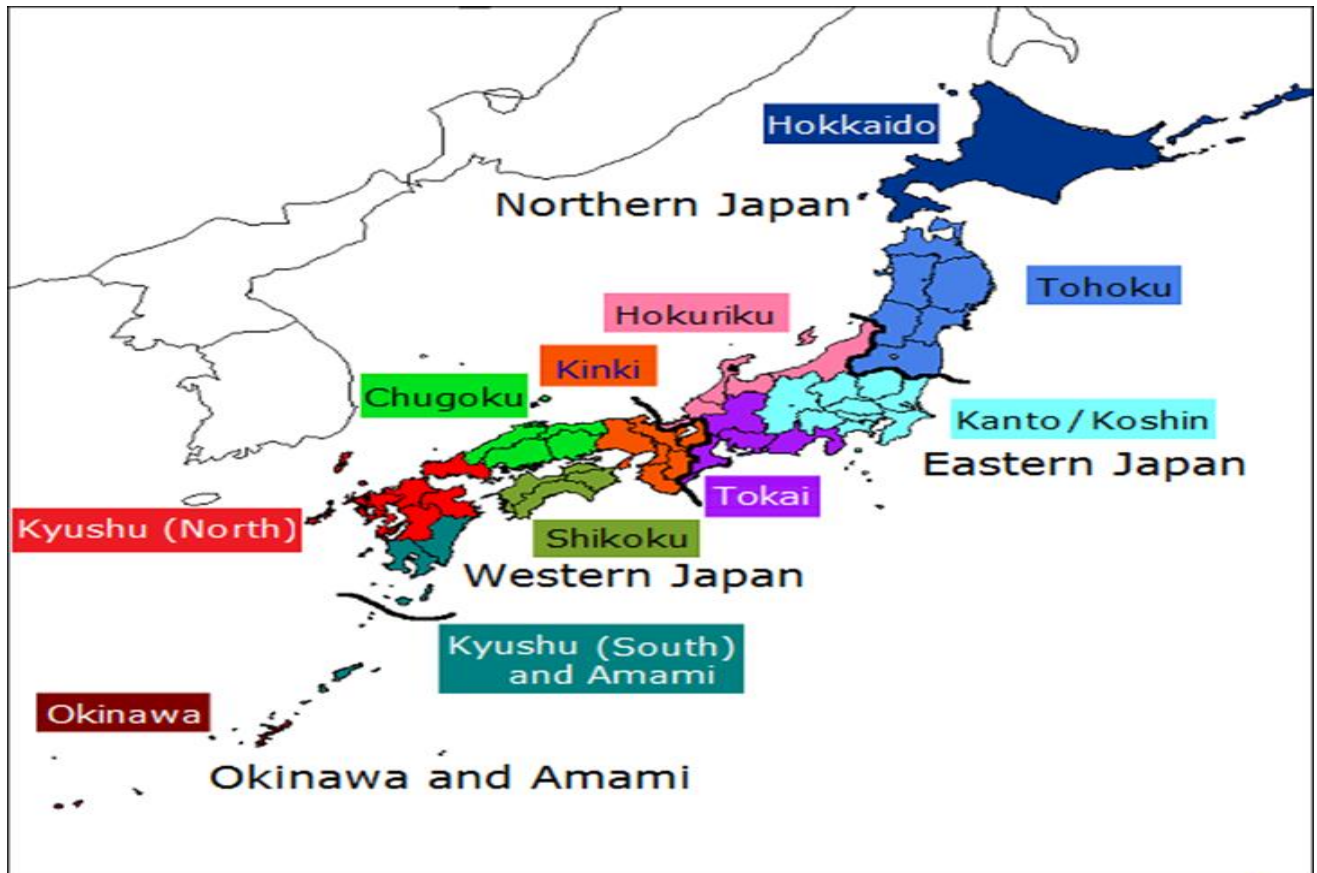


Figure 1 (Source: Ministry of the Environment, Japan, 2020)

Kyoto

Kyoto is a city in Japan that has a temperate marine climate, which differs by region depending on the effects of seasonal winds and ocean currents. The northwest monsoon in the winter brings humid conditions with heavy precipitation (snow) to the Sea of Japan side of Honshu but comparatively dry weather with low precipitation to the Pacific Ocean side. In the summer, the

southeast monsoon brings high temperatures and low rainfall on the Sea of Japan side, and high temperatures and high humidity on the Pacific Ocean side. Climate change poses a significant threat to Kyoto and other regions around the world. The impacts of climate change can include more frequent and severe weather events, rising sea levels, and changes in precipitation patterns. The summers in Kyoto are short, hot, oppressive, and mostly cloudy, while the winters are very cold, windy, and partly cloudy. The city experiences significant seasonal variation in the percentage of the sky covered by clouds, with the clearer part of the year beginning around September 16 and lasting for 6.6 months, ending around April 3. The clearest month of the year in Kyoto is December, during which on average the sky is clear, mostly clear, or partly cloudy 71% of the time. The cloudier part of the year begins around April 3 and lasts for 5.4 months, ending around September 16. This city experiences two long spells of rainy seasons, one in early summer when the southeast monsoon begins to blow, and the other in autumn when the winds cease. The wetter season lasts 3.3 months, from June 13 to September 24, with a greater than 40% chance of a given day being a wet day. The month with the most wet days in Kyoto is July, with an average of 13.7 days with at least 0.04 inches of precipitation. The drier season lasts 8.7 months, from September 24 to June 13. The month with the fewest wet days in Kyoto is November, with an average of 8.5 days with at least 0.04 inches of precipitation. Kyoto experiences soaring temperatures and high subtropical humidity during the summer and typhoon season in the fall. Overall, Kyoto's climate and weather experience significant seasonal variation, with distinct differences in temperature, precipitation, and cloud cover throughout the year. Figure (2) and Figure (3) show the case study and seasonal variation of meteorological elements in this city, respectively.

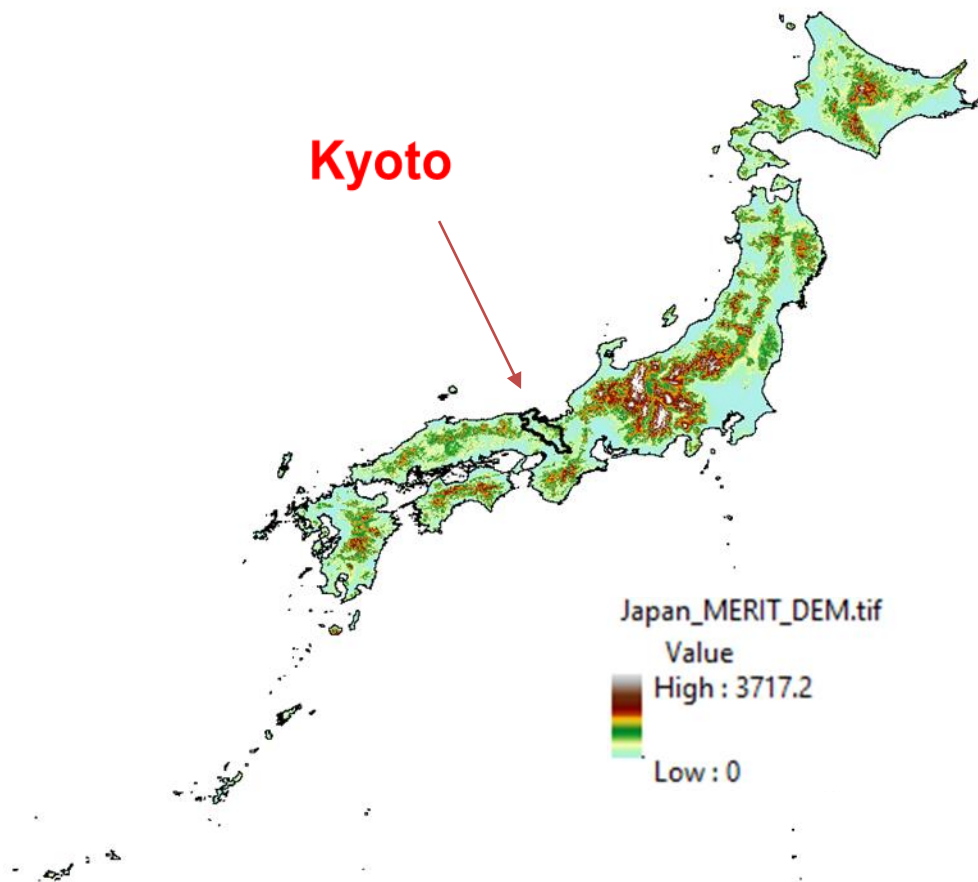


Figure (2). Case study (Source: Ministry of the Environment, Japan, 2020)

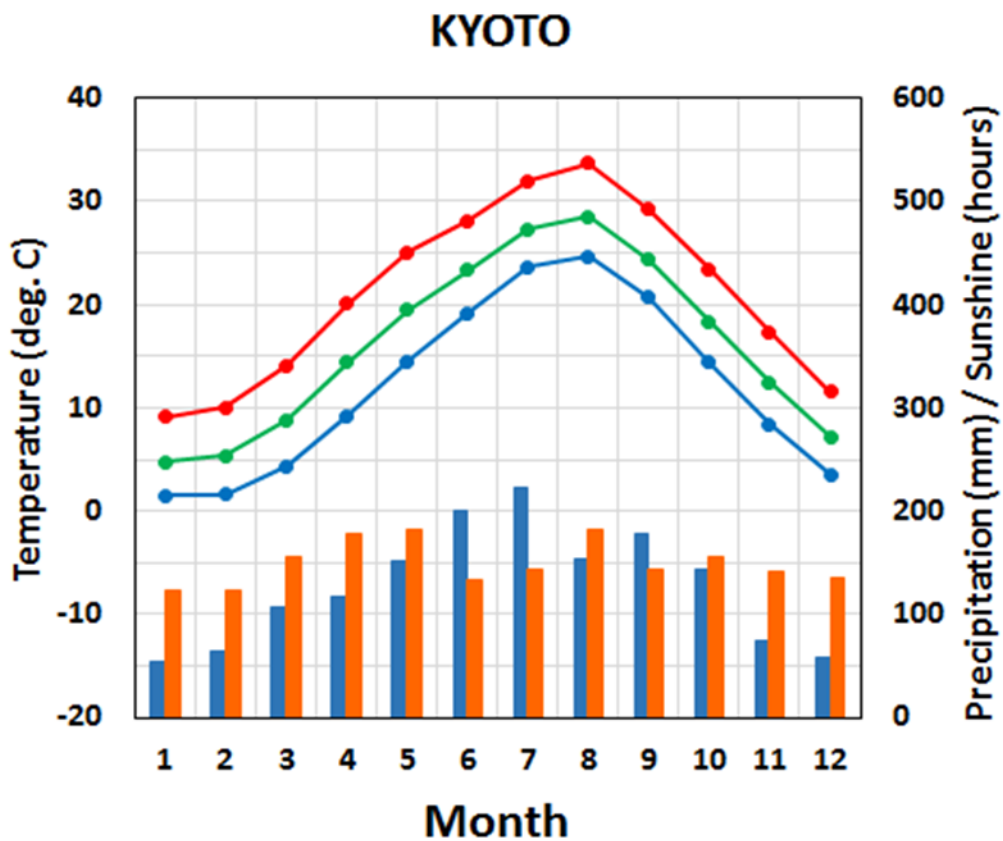


Figure (3). Seasonal variation of meteorological elements in Kyoto

(Source: Ministry of the Environment, Japan, 2020)

2. Materials and Methods

2.1. Fuzzy logic model

The FL approach is an appropriate way to handle complicated and ambiguous problems and improve the integration of multiple variables of future estimations. The FL model transforms input data into output using fuzzy set theory (Zadeh, 1965). Fuzzy sets allow partial membership ranging from 0 to 1. In order to overcome intrinsic ambiguity, fuzzy sets are represented by Membership Functions (MFs) with ambiguous bounds and progressive transitions between defined sets (Gutiérrez-Estrada et al., 2004). As a result, the FL is well adapted to estimating environmental, hydrogeological, and hydrological factors (e.g., precipitation) subject to uncertainty and ambiguity (Olatunji et al., 2011; Asadi et al., 2014). The FL model comprises three main components: fuzzification, fuzzy rule-based inference, and defuzzification. The main goal of the fuzzification process is to discover a model structure that contains the appropriate number of rules and data clusters. Researchers employed various clustering approaches to identify the structure (Hathaway & Bezdek, 1988; Bezdek, 1981; Chiu, 1994). Fuzzy clustering was used to find patterns in large datasets representing specific system characteristics. The fuzzy sets are created after data clustering, which are then used to build the inference engine using various MFs (e.g., trapezoidal, triangular, Gaussian, sigmoid). Rules are the basis of the inference engine. Each rule comprises multiple inputs leading to one or more outputs. In order to connect the antecedents of fuzzy rules that incorporate more than one rule, four fuzzy operators were used: OR (maximum), AND (minimum), prod (product), and NOT. This takes a single integer from the antecedent as input and produces a fuzzy set as output. Since all the rules in the FL model must be tested before making a decision, the rules must be aggregated using aggregation processes. Finally, defuzzification is the process of converting an aggregation result into a crisp output. The output MFs in the FL approach are fuzzy sets. After the aggregation procedure, each output variable has a fuzzy set that must be fuzzified (Mamdani & Assilian, 1975; Mamdani, 1977). The fuzzy model can be applied by

Mamdani Fuzzy Logic (MFL) (Mamdani & Assilian, 1975; Mamdani, 1977) and Sajo Fuzzy Logic (SFL) (Sugeno, 1985) methods. Mamdani and Assilian introduced the Mamdani fuzzy inference system in 1975 (Mamdani & Assilian, 1975). It is based on nonlinear algorithms for complex systems and decision-making processes. In 1985, Sugeno introduced another fuzzy inference system similar to the Mamdani method (Sugeno, 1985). The first part of the fuzzy inference process, which is the fuzzification of the inputs and the implementation of fuzzy operators, is the same in both the Mamdani and Sajo methods. The main difference is their output. In the Sajo method, the system's output is a fixed function or a linear relationship obtained by the classification method. However, the Mamdani inference system uses fuzzy sets as the result of the rules, and the output of each rule is nonlinear and fuzzy. Mamdani's method expresses logical results with a relatively simple structure, primarily utilized in decision-making processes and systems interpreting laws. The advantage of the Mamdani method is its intuitiveness; Hence, it is more common than the Sajo method.

2.2. Z-number concept description

The Z-number represents information reliability and is used to conduct computations based on unreliable information. Generally, a Z-number consists of two fuzzy numbers defined by $Z = (A, B)$. The first part, A, determines the constraint for the uncertain parameter X. The second part, B, denotes the reliability of the first part. Most known methods have concentrated on converting Z-numbers to fuzzy numbers for calculations on such linguistic parameters. The Z-numbers can be combined using one of three different methods as follows:

- i) Simple procedures to convert Z-numbers to fuzzy numbers and integrate them (Kang et al., 2018).
- ii) The separate aggregation of parts A and B (Glukhoded and Smetanin, 2016).
- iii) Calculating Z^+ -number, combining Z^+ -numbers, and calculating Z-number using calculated Z^+ -number (Aliev et al., 2015, 2016).

While the first and second approaches are simple to understand and use, they do not work for all fuzzy numbers and may lose some information. The information loss is minimized in the third approach, but it is difficult and needs nonlinear optimization methods (Glukhoded and Smetanin,

2016). This research focused on developing MATLAB code based on simplifying the third approach to make it practical. The rules are weighted based on fuzzy Hausdorff distances in this simplified method. Following is a brief discussion of the Z-number definitions.

2.2.1. Z-valued if-then rules based reasoning

Z-interpolation, which involves interpolating Z-rules, has been discussed by Zadeh (2011). The expansion of fuzzy rule interpolation is the solution to this problem (Kóczy & Hirota, 1991).

Considering the n Z-rules below:

If X_1 is $Z_{X1,1} = (A_{X1,1}, B_{X1,1})$ and ... and X_m is $Z_{Xm,1} = (A_{Xm,1}, B_{Xm,1})$, then Y is $Z_Y = (A_{Y,1}, B_{Y,1})$.

If X_1 is $Z_{X1,2} = (A_{X1,2}, B_{X1,2})$ and ... and X_m is $Z_{Xm,2} = (A_{Xm,2}, B_{Xm,2})$, then Y is $Z_Y = (A_{Y,2}, B_{Y,2})$.

...

If X_n is $Z_{X1,n} = (A_{X1,n}, B_{X1,n})$ and ... and X_m is $Z_{Xm,n} = (A_{Xm,n}, B_{Xm,n})$, then Y is $Z_Y = (A_{Y,n}, B_{Y,n})$.

and a current observation as:

X_1 is $Z'_{X1} = (A'_{X1}, B'_{X1})$ and ... and X_m is $Z'_{Xm} = (A'_{Xm}, B'_{Xm})$,

It is helpful to discover the observation's Z-value of $Y(Z'_Y)$. There are (n) rules and (m) Z-valued input variables.

The output Z'_Y of Z-rules was determined as follows:

$$Z'_Y = \sum_{j=1}^{nn} w'_j \cdot Z_{Y,j} = \sum_{j=1}^{nn} w'_j (A_{Y,j}, B_{Y,j}) \quad (1)$$

where,

$$w'_j = (w_j) / (\sum_{j=1}^{nn} w_j), \text{ in which, (nn) indicates the number of chosen rules (rules with high} \quad (2)$$

weight),

$$w_j = (1/\rho_j) / (\sum_{j=1}^n 1/\rho_j), \quad j = 1, \dots, n \quad (3)$$

$$\rho_j = \sum_{i=1}^m D(Z'_{Xi}, Z_{Xi,j}) \quad (4)$$

$$D(Z_1, Z_2) = d(A_1, A_2) + d(B_1, B_2), \quad (5)$$

where,

$$d(A_1, A_2) = \sup \{d_H(A_1^\alpha, A_2^\alpha) \mid 0 < \alpha \leq 1\}, \text{ in which, } d_H \text{ represents fuzzy Hausdorff distance,} \quad (6)$$

$$d_H(A_1, A_2) = \bigcup_{\alpha \in [0,1]} \alpha d_H^\alpha(A_1, A_2). \quad \text{where U represents the unions of classic sets.} \quad (7)$$

Where there are (n) Z-rules, Z_j represents the Z-number valued consequent of the jth rule, w_j , $j=1, \dots, n$ are linear interpolation coefficients. In the jth rule, D represents the distance between the present i th Z-number valued input and antecedent. Therefore, the distance between the input vector and the jth rule's antecedents is calculated using ρ . The weights are assigned to the rules (according to Equations 3-7), and the most efficient rules are used in Equation 1. In order to conform to the superposition concept ($w'_1 + w'_2 + \dots + w'_{nn} = 1$), it is necessary to reweight the selected rules using Equation (2). Despite the little negative effect of a single low-weight rule, adding many low-weight rules at once can significantly decrease performance. Therefore, the adopted method in this paper chooses only high-weight rules (at least 0.9 of their maximum weight).

It is important to multiply the weights of the chosen rules by the Z-numbers. In this case, $Z_y = \lambda \cdot Z_x(A_x, B_x)$ is calculated as $Z_y = Z_x(\lambda \cdot A_x, B_x)$. It means multiplying by λ does not affect the reliability part of the Z-number (B_x).

As a result, the discrete fuzzy number A can be multiplied by an actual number $\lambda \in \mathbb{R}$, to generate a discrete fuzzy number $A_1 = \lambda A$. Its α -cut is explained as (Aliiev et al., 2016, 2015):

$$A_1^\alpha = \{x \in \lambda \cdot \text{supp}(A) \mid \min(\lambda A^\alpha) \leq x \leq \max(\lambda A^\alpha)\} \quad (8)$$

Where:

$$\lambda \cdot \text{supp}(A) = \{\lambda x \mid x \in \text{supp}(A)\}$$

$$\min(\lambda A^\alpha) = \min\{\lambda x \mid x \in A^\alpha\} \quad (9)$$

$$\max(\lambda A^\alpha) = \max\{\lambda x \mid x \in A^\alpha\}$$

And the membership function was described as:

$$\mu_{\lambda A}(x) = \sup\{\alpha \in [0, 1] \mid x \in (\lambda A^\alpha)\} \text{ where sup represents the supremum or max.} \quad (10)$$

2.3. Proposed methodology

The flowchart of the proposed methodology is demonstrated in Fig. 4a. Also, Fig.4b. shows the topographical condition of the region, and Fig. 2c shows an example of the occurrence of extreme events in western japan (heavy precipitation). The proposed methodology in the current study contains four distinct steps (i.e., data pre-processing, extraction of the association rules, modeling by Z-number and conventional fuzzy tools, and finally, comparing and evaluating the obtained results) using ocean-atmospheric signals time series to predict the occurrence of considered extreme weather events.

In the first step, the hydro-climatic signals as predictors and considered extreme weather events as predictands are classified into some classes (by evaluating different methods). In the second step, the association rule mining method is used to discover the patterns among the hydro-climatic signals and considered extreme weather events datasets to construct if-then rules. In the third step, conventional fuzzy and Z-number-based modeling are applied to the patterns found in the second step. Therefore, if-then rules were constructed, and then the modeling was conducted. Finally, in the fourth step, the results of both methods (classic fuzzy and Z-number) are evaluated and compared based on the efficiency criteria used.

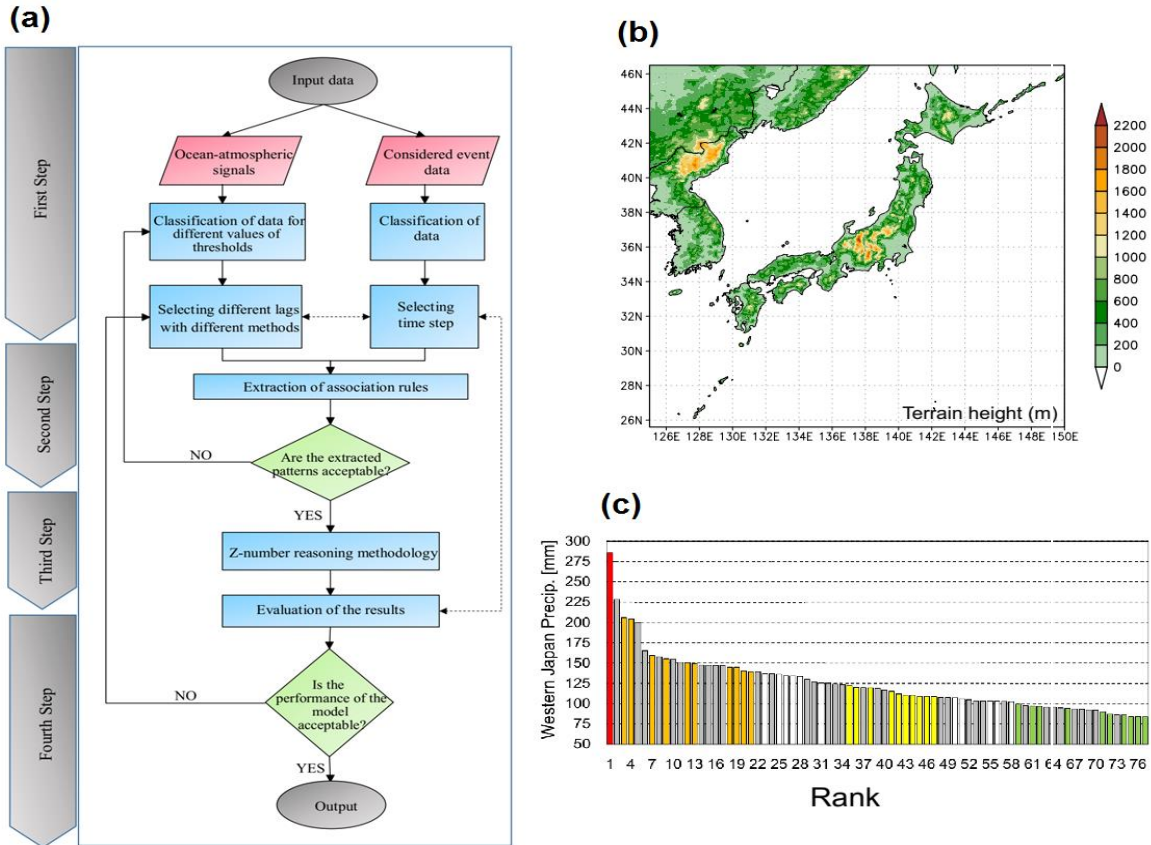


Fig. 4: **a)** Flowchart depicting the Z-number reasoning methodology, **b)** Topographic map of Japan and **c)** Rank of heavy 3-day precipitation averaged (exceeds the 95th percentile) over western Japan during the warm seasons (May-September) from 1979 to 2018.

2.4. Evaluation criteria

Traditional evaluation criteria like Nash–Sutcliffe efficiency (NSE) and Root Mean Square Error (RMSE) can be used to assess numerical point prediction outputs. However, they are unsuitable for evaluating model performance (Sharghi et al., 2021). The outputs from this study are divided into five classes, so Heidke Skill Score (HSS) and Total Accuracy (TA) were employed to evaluate the outputs (Moreira, 2016). The TA criterion involves computing the ratio of correct predictions to total predictions made. An ideal model would achieve a TA value of 100%. It can be calculated using the following formula:

$$TA = \frac{(TVH+TH+TM+TL+TVL)}{n} \times 100 \quad (14)$$

Furthermore, in this research, the HSS metric was employed to evaluate the performance of the models. HSS compares the accuracy of the forecasts with the accuracy that would be expected by chance. For models with (I) forecasts and occurrences, HSS is defined as follows (Wilks, 2011):

$$HSS = \frac{\sum_{i=1}^I p(y_i, o_i) - \sum_{i=1}^I p(y_i) \cdot p(o_i)}{1 - \sum_{i=1}^I p(y_i) \cdot p(o_i)} \quad (15)$$

$p(y_i)$ and $p(o_i)$ are the probability distributions for the estimations and observations, respectively. This criteria ranges from $-\infty$ to 1.

3. Result

It is worth noting that the association rule technique treats the linguistic terms as intervals, but these interval sets must be transformed into fuzzy sets for fuzzy logic-based modeling. As mentioned, data were classified using $(\mu \pm i\sigma)$ in which $(i= 0.5,1,1.5)$. Figure (5) shows the data categorization, including SST-Sea of Japan, SST-Yellow Sea, SST-East Sea, min temperature of Japan, SOI, ONI-sst, ENSO, precipitation, and snow depth.

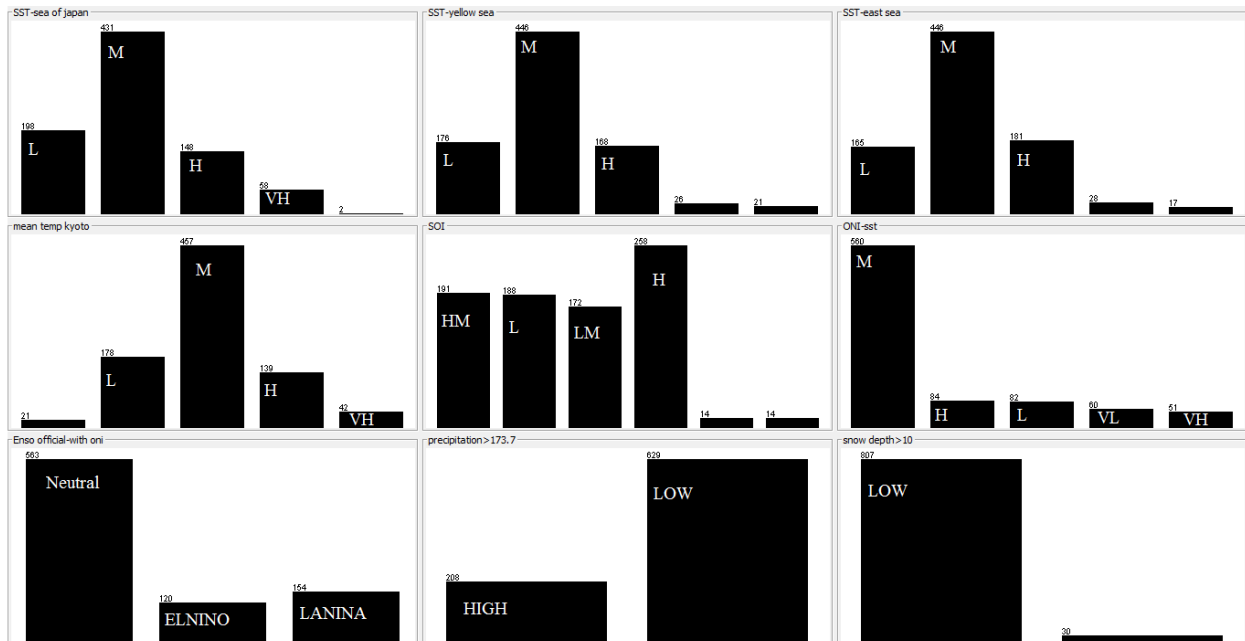


Figure (5). Data categorization.

In this study, 6000 patterns extracted using data mining techniques with confidence >0.5 . For Examples (for predicting 5 months ahead):

1- SST (east sea)=H, ONI (SST)=M (139 times) \implies precipitation (t+5) <173.7 mm (139 times) conf:(1).

2- SST (sea of Japan)=L, SST (Yellow sea)=L, mean temp Kyoto=L, SOI=LM, ONI (SST),=M, ENSO=El-Nino (9 times) \implies precipitation (t+5) >173.7 (9 times) conf:(1).

3- SST (sea of Japan)=VH, SST (Yellow sea)=VH, SST (East sea=VH), SOI=H (4 times) \implies snow depth >10 (2 times) conf:(0.5).

It is recommended for future works to conduct more studies about the climate of Japan, examine more inputs, develop a model for two more stations, and prepare reports and papers.

3. References

Aboutorab, H., Saberi, M., Asadabadi, M.R., Hussain, O. and Chang, E., 2018. ZBWM: The Z-number extension of Best Worst Method and its application for supplier development. *Expert Systems with Applications*, 107, pp. 115-125.

Akbarian Saravi, N., Yazdanparast, R., Momeni, O., Heydarian, D. and Jolai, F., 2018. Location optimization of agricultural residues-based biomass plant using Z-number DEA. *Journal of Industrial and Systems Engineering*, 12(1), pp.39-65.

Aliiev, R.A., Huseynov, O.H., Aliyev, R.R., Alizadeh, A.A., 2015. *The arithmetic of Z-numbers: Theory and applications*. World Scientific, Singapore.

Aliiev, R.A., Pedrycz, W., Huseynov, O.H., Eyupoglu, S.Z., 2016. Approximate Reasoning on a Basis of Z-Number-Valued If-Then Rules. *IEEE Transactions on Fuzzy Systems* 25, pp.1589–1600.

Asadi, S., Hassan, M., Nadiri, A. and Dylla, H., 2014. Artificial intelligence modeling to evaluate field performance of photocatalytic asphalt pavement for ambient air purification. *Environmental Science and Pollution Research*, 21(14), pp.8847-8857.

Bezdek, J.C., 1981. Objective function clustering. In *Pattern recognition with fuzzy objective function algorithms*. Springer, Boston, MA, pp. 43-93.

Chiu, S.L., 1994. Fuzzy model identification based on cluster estimation. *Journal of Intelligent & fuzzy systems*, 2(3), pp.267-278.

- Dadaser-Celik, F., Celik, M., Dokuz, A., 2013. Associations between stream flow and climatic variables at Kizilirmak river basin in Turkey. *Global NEST Journal* 14, pp.354–361.
- Dhanya, C.T., Nagesh Kumar, D., 2009. Data mining for evolution of association rules for droughts and floods in India using climate inputs. *Journal of Geophysical Research: Atmospheres* 114, pp.1–15.
- Ghasemi, A.R., Khalili, D., 2008. The association between regional and global atmospheric patterns and winter precipitation in Iran. *Atmospheric Research* 88, pp.116–133.
- Glukhoded, E.A., Smetanin, S.I., 2016. The method of converting an expert opinion to Z-number. *Proceedings of the Institute for System Programming of the RAS* 28, pp.7–20.
- Gutiérrez-Estrada, J.C., de Pedro-Sanz, E., López-Luque, R. and Pulido-Calvo, I., 2004. Comparison between traditional methods and artificial neural networks for ammonia concentration forecasting in an eel (*Anguilla anguilla* L.) intensive rearing system. *Aquacultural Engineering*, 31(3-4), pp.183-203.
- Hathaway, R.J. and Bezdek, J.C., 1988. Recent convergence results for the fuzzy c-means clustering algorithms. *Journal of Classification*, 5(2), pp.237-247.
- He, Y., Yan, Y., Wang, X. and Wang, C., 2019. Uncertainty forecasting for streamflow based on support vector regression method with fuzzy information granulation. *Energy Procedia*, 158, pp.6189-6194.
- Kang, B., Deng, Y., Hewage, K., Sadiq, R., 2018. A method of measuring uncertainty for Z-number. *IEEE Transactions on Fuzzy Systems* 27, pp.731–738.
- Kóczy, L.T., Hirota, K., 1991. Rule interpolation by α -level sets in fuzzy approximate reasoning. *J. BUSEFAL, Automne, URA-CNRS* 46, pp.115–123.
- Kosaka, Y., Nakamura, H., 2010. Mechanisms of meridional teleconnection observed between a summer monsoon system and a subtropical anticyclone. Part I: The Pacific–Japan pattern. *J. Clim.* 23, pp.5085–5108.
- Maleki, S., Nourani, V., Najafi, H., Baghanam, A.H. and Ke, C.Q., 2023. Z-numbers based novel method for assessing groundwater specific vulnerability. *Engineering Applications of Artificial Intelligence*, 122, p.106104.
- Mamdani, E.H, Assilian, S., 1975. An experiment in linguistic synthesis with a fuzzy logic controller. *International Journal of Man-machine Studies*, 7, pp.1–13.
- Mamdani, E.H., 1977. Application of fuzzy logic to approximate reasoning using linguistic synthesis. *IEEE transactions on computers*, 26(12), pp.1182-1191.
- Meidani, E., Araghinejad, S., 2014. Long-lead streamflow forecasting in the southwest of Iran by sea surface temperature of the Mediterranean Sea. *Journal of Hydrologic Engineering* 19, pp.5014005.
- Moreira, E.E., 2016. SPI drought class prediction using log-linear models applied to wet and dry seasons. *Phys. Chem. Earth, Parts A/B/C* 94, 136–145.

- Moser, S.C., Hart, J.A.F., 2015. The long arm of climate change: societal teleconnections and the future of climate change impacts studies. *Climatic Change* 129, 13–26.
- Najafi, H., Nourani, V., Sharghi, E., Roushangar, K. and Dąbrowska, D., 2022. Application of Z-numbers to teleconnection modeling between monthly precipitation and large scale sea surface temperature. *Hydrology Research*, 53(1), pp.1-13.
- Nourani, V., Najafi, H., Sharghi, E., Roushangar, K., 2021. Application of Z-Numbers to monitor drought using large-scale oceanic-atmospheric parameters. *Journal of Hydrology* 598, pp.126198.
- Nourani, V., Tahershamsi, A., Abbaszadeh, P., Shahrabi, J. and Hadavandi, E., 2014. A new hybrid algorithm for rainfall–runoff process modeling based on the wavelet transform and genetic fuzzy system. *Journal of Hydroinformatics*, 16(5), pp.1004-1024.
- Ohba, M., Sugimoto, S., 2021. Dynamic and thermodynamic contributions of ENSO to winter precipitation in Japan: frequency and precipitation of synoptic weather patterns. *Clim. Dyn.* pp.1–16.
- Olatunji, S.O., Selamat, A. and Abdulraheem, A., 2011. Modeling the permeability of carbonate reservoir using type-2 fuzzy logic systems. *Computers in Industry*, 62(2), pp.147-163.
- Sharghi, E., Paknezhad, N.J., Najafi, H., 2021. Assessing the effect of emotional unit of emotional ANN (EANN) in estimation of the prediction intervals of suspended sediment load modeling. *Earth Sci. Inform.* 14 (1), 201–213.
- Stefan, S., Ghioca, M., Rimbu, N., Boroneant, C., 2004. Study of meteorological and hydrological drought in southern Romania from observational data. *International Journal of Climatology* 24, pp.871–881.
- Sugeno M (1985) An introductory survey of fuzzy control. *Information sciences*, 36(1-2), pp.59-83.
- Tadesse, T., Wilhite, D.A., Harms, S.K., Hayes, M.J. and Goddard, S., 2004. Drought monitoring using data mining techniques: A case study for Nebraska, USA. *Natural Hazards*, 33(1), pp.137-159.
- Webster, P.J., Magana, V.O., Palmer, T.N., Shukla, J., Tomas, R.A., Yanai, M.U., Yasunari, T., 1998. Monsoons: Processes, predictability, and the prospects for prediction. *Journal of Geophysical Research: Oceans* 103, pp.14451–14510.
- Wilks, D.S., 2011. *Statistical methods in the atmospheric sciences* (Vol. 100). Academic press.
- Ying, J., Huang, P., Lian, T., 2019. Changes in the sensitivity of tropical rainfall response to local sea surface temperature anomalies under global warming. *International Journal of Climatology* 39, pp.5801–5814.
- Zadeh, L.A., 1965. Electrical engineering at the crossroads. *IEEE Transactions on Education*, 8(2), pp.30-33.
- Zadeh, L.A., 2011. A note on Z-numbers. *Inform. Sci.* 181 (14), 2923–2932.
- Zadeh, L.A., 2011. A note on Z-numbers. *Information Sciences*, 181(14), pp.2923-2932.